Available online at www.sciencedirect.com

SCIENCE DIRECT

Biochimica et Biophysica Acta 1669 (2005) 34–42

BIOCHIMICA ET BIOPHYSICA ACTA
BBA

http://www.elsevier.com/locate/bba

# Epithelial transport and barrier function in *occludin*-deficient mice

J.D. Schulzke[a,*], A.H. Gitter[b,c], J. Mankertz[a], S. Spiegel[d], U. Seidler[d], S. Amasheh[b], M. Saitou[e], S. Tsukita[e], M. Fromm[b]

[a]*Department of Gastroenterology, Campus Benjamin Franklin, Charité - Universitary Medicine Berlin, Germany*
[b]*Department of Clinical Physiology, Campus Benjamin Franklin, Charité - Universitary Medicine Berlin, Germany*
[c]*Department of Medical Engineering, Jena University of Applied Sciences, Carl-Zeiss-Promenade 2, Jena, Germany*
[d]*Med. Klinik, Medizinische Hochschule Hannover, Germany*
[e]*Department of Cell Biology, Kyoto University Faculty of Medicine, Japan*

Received 9 June 2004; received in revised form 14 December 2004; accepted 13 January 2005
Available online 1 February 2005

**Abstract**

*Background and Aims*: This study aimed at functional characterization of the tight junction protein *occludin* using the *occludin*-deficient mouse model.
*Methods*: Epithelial transport and barrier functions were characterized in Ussing chambers. Impedance analysis revealed the ionic permeability of the epithelium ($R^e$, epithelial resistance). *Conductance scanning* differentiated transcellular ($G^c$) and tight junctional conductance ($G^{tj}$). The pH-stat technique quantified gastric acid secretion.
*Results*: In *occludin*+/+ mice, $R^e$ was 23±5 Ω cm$^2$ in jejunum, 66±5 Ω cm$^2$ in distal colon and 33±6 Ω cm$^2$ in gastric corpus and was not altered in heterozygotic *occludin*+/− or homozygotic *occludin*−/− mice. Additionally, [$^3$H]mannitol fluxes were unaltered. In the control colon, $G^c$ and $G^{tj}$ were 7.6±1.0 and 0.3±0.1 mS/cm$^2$ and not different in *occludin* deficiency. Epithelial resistance after mechanical perturbation or EGTA exposition (low calcium switch) was not more affected in *occludin*−/− mice than in control. Barrier function was measured in the urinary bladder, a tight epithelium, and in the stomach. Control $R^t$ was 5.8±0.8 kΩ cm$^2$ in urinary bladder and 33±6 Ω cm$^2$ in stomach and not altered in *occludin*−/− mice. In gastric corpus mucosa, the glandular structure exhibited a complete loss of parietal cells and mucus cell hyperplasia, as a result of which acid secretion was virtually abolished in *occludin*−/− mice.
*Conclusion*: Epithelial barrier characterization in *occludin*-deficiency points against an essential barrier function of *occludin* within the tight junction strands or to a substitutional redundancy of single tight junction molecules like *occludin*. A dramatic change in gastric morphology and secretory function indicates that *occludin* is involved in gastric epithelial differentiation.


*Keywords:* Tight junction; Occludin; Impedance analysis; Conductance scanning; Gastric acid secretion

## 1. Introduction

To maintain vectorial transport epithelial cells are equipped with tight junctions to separate the paracellular space from the intestinal lumen. Tight junction structure has been studied by EM, especially with the freeze fracture technique. Most epithelial tight junctions are equipped with 4–9 horizontally-oriented strands varying in complexity with organ and segment and there seems to be a logarithmic correlation between resistance and strands

*Abbreviations:* AC, alternating current; $I_{SC}$, short-circuit current; $R^t$, total tissue resistance; $R^e$, resistance of the epithelial layer; $R^{sub}$, resistance of the subepithelial tissues; $G^t$, total tissue conductivity; $G^{se}$, conductivity of the surface epithelium; $G^{cry}$, conductivity of the crypts; $G^c$, conductivity of the transcellular pathway; $G^{tj}$, conductivity of the paracellular (i.e. tight junctional) pathway; NS, not significant

* Corresponding author. Medizinische Klinik I, Charité, Campus Benjamin Franklin 12200 Berlin, Germany. Tel.: +49 30 8445 2666; fax: +49 30 8445 4493.
*E-mail address:* joerg.schulzke@charite.de (J.D. Schulzke).

0005-2736/$ - see front matter © 2005 Elsevier B.V. All rights reserved.
doi:10.1016/j.bbamem.2005.01.008

number [1]. Finally, the tight junction is not a static extracellular domain but can undergo rapid regulatory changes e.g. in response to inflammation [2] or cAMP [3], complement factors [4], and vibrio cholerae enterotoxin [5].

Only about 10 years ago, *occludin* was the first protein identified as strand-forming component in a membrane fraction obtained from chicken liver [6,7]. While 24 *claudins* [8,9] and junction associated molecules (*JAM*) 1–3 [10] have been recognized as tight junction strand constituents, the functional role of *occludin* is still far from being clear. Experimental approaches include *occludin* over-expression or functional inactivation by blocking its interaction with other tight junction molecules (cf. Discussion). Another direct approach comprises *occludin*-deficient stem cells [11] and the *occludin* knock out mouse [12]. Morphological characterization of *occludin*-deficiency pointed to growth retardation and chronic gastritis, while preliminary electrophysiological data did not reveal a great change in barrier function as indicated by overall epithelial resistances in small or large intestine. The present study aimed to functionally characterize its epithelial transport and barrier function in more detail. For this purpose, conventional Ussing measurements of electrogenic transport (short circuit current; $I_{SC}$) and electrical resistance ($R^t$) including tracer flux measurements with [$^3$H]mannitol and $^{22}$Na were performed as well as alternating current impedance analysis, to separate epithelial resistance from that of the underlying subepithelium [13–15]. To exclude that changes in cellular membrane permeability compensate for altered tight junction permeability, the *conductance scanning* method was applied which differentiates trans- and paracellular conductances [16]. In addition, tight junctions were characterized under mechanical stress and EGTA (low calcium switch), to detect whether *occludin*-deficient tight junctions are more “fragile” than control tight junctions.

As the main important finding *occludin*-deficient mice did not show an epithelial barrier defect. Instead of barrier defects, a significant reduction in active transport was observed, namely in electrogenic transport of the small intestine and in gastric acid secretion which was paralleled by a defect in parietal cell differentiation. This suggests a potential role of *occludin* in signal transduction pathways involved in epithelial transport and/or tissue growth and differentiation.

## 2. Materials and methods

### 2.1. Occludin knock out mice

Homo- and heterozygotic *occludin*-deficient mice were obtained as described previously [12]. BW was 34±2 g ($n$=8) in control, 35±1 g ($n$=9) in *occludin*+/− and 27±1 g ($n$=10; $p<0.01$ versus control) in *occludin*−/− mice.

### 2.2. Tissue preparation

Measurements were performed at week 52 on jejunum, distal colon, gastric corpus and urinary bladder. Specimens were used without stripping of the muscle layer(s), except the stomach. Gastric tissue was spread mucosal side down and the muscularis and submucosa were removed with scissors exposing the base of the glands.

### 2.3. Solutions and drugs

The fluid composition was (mM): $Na^+$ 140, $Cl^-$ 123.8, $K^+$ 5.4, $Ca^{2+}$ 1.2, $Mg^{2+}$ 1.2, $HPO_4^{2-}$ 2.4, $H_2PO_4^-$ 0.6, $HCO_3^-$ 21, D(+)-glucose 10, β-OH-butyrate 0.5, glutamine 2.5, and D(+)-mannose 10, gassed with 95% $O_2$ and 5% $CO_2$, pH was 7.4 at 37 °C [14]. Azlocillin and Tobramycin were used at 50 mg/l and 4 mg/l which had no known $I_{SC}$ or $R^t$ effect [17,18]. [$^3$H]mannitol and $^{22}$Na were from Du Pont de Nemours, Wilmington, USA.

### 2.4. Short circuit current ($I_{SC}$), transepithelial resistance and sodium and mannitol tracer flux measurements

Ussing-experiments were performed under short circuited conditions as described previously [14,18]. Tissue area was 0.28 cm$^2$. $I_{SC}$ was corrected for bath resistance [17]. Resistance of urinary bladder was determined in the *conductance scanning* chamber, where the microelectrode above the tissue approached the mucosal surface at 50 μm. All conductivities and resistances are referred to the gross tissue area (0.28 cm$^2$). Mannitol permeability was determined as mucosal-to-serosal [$^3$H]mannitol flux.

### 2.5. Alternating current (AC) impedance analysis

AC impedance analysis discriminates epithelial ($R^e$) and subepithelial ($R^{sub}$) resistance [14,15,17]. Voltage responses to sine-wave alternating current of 48 frequencies (1 Hz–65 kHz, 35 μA/cm$^2$ eff.) were detected by phase-sensitive amplifiers (Model 1250 and 1286; Solartron Schlumberger, Farnborough Hampshire, GB). Complex impedance values were corrected for the resistance of the bathing solution. Impedance loci were plotted in Nyquist diagrams and circle segments were fitted by least square analysis. The elevation of center points of circle segments above the abscissa indicates more than one RC-unit to be present in the epithelium, the capacitances of which merge to an apparent one [15]. This is due to different cell types in the epithelium and its complex architecture. For differentiation of epithelial and subepithelial resistance, the extrapolation of the measured data to the abscissa at the low-frequency end ($R^t$) and at the high-frequency end ($R^{sub}$) was used ($R^e=R^t-R^{sub}$).

### 2.6. Conductance scanning measurements

To differentiate crypt and surface contributions to epithelial conductivity, medium resolution *conductance scanning* was applied [19,20]. Trans- and paracellular pathways were distinguished by high resolution *conductance scanning* [16]. In brief, mouse distal colon was mounted in horizontal Ussing chambers (viewed through a 20–40× water-immersion object lens). Alternating current (AC, 0.2 mA×cm$^{-2}$, 24 Hz) was clamped across the epithelium and the electric field generated in the mucosal bath solution was measured with a microelectrode probe above the epithelial surface. With the electric field measured and the specific resistivity of the solution, the local current density was calculated [19]. This and the transepithelial voltage yielded the local conductivity.

### 2.7. Epithelial barrier function during mechanical stress and calcium depletion

Standardized mechanical perturbation of the large intestinal was performed as described previously [21]. Distension of the intestine was applied by periodically aspirating and re-injecting 0.1 ml of serosal bathing fluid with a syringe which caused visible bulging of the tissue (suction cycles at about 2 Hz for 20 s). Chemical perturbation of tight junctions was performed by lowering the calcium concentration by 1.5 mM EGTA.

### 2.8. Ussing experiments in gastric mucosa

Mucosa was mounted in 0.63 cm$^2$ Ussing chambers of oval shape. TTX ($10^{-6}$ mM, to abolish neuronal influences) and indomethacin ($3\times10^{-5}$ M, against prostaglandins) were serosally added. Open-circuit transepithelial electrical potential difference (PD) was recorded via agar 3 M KCl bridges. The direct-current electrical resistance was determined from the change in PD after sending a 40 μA/cm$^2$ current (200 ms in either direction). $I_{SC}$ was calculated from PD and resistance. Luminal pH was maintained at 7.4 by a continuous pH stat titration method (Radiometer, Copenhagen, Denmark).

### 2.9. Analysis of occludin gene products

Tissue was extracted with RNAzol (WAK Chemie, Germany). RNA was precipitated with isopropanol and subjected to UV spectrophotometry. First strand cDNA was generated with 50 units murine leucemia virus reverse transcriptase, 5 mM $MgCl_2$, PCR buffer II (Perkin-Elmer), 40 U RNase inhibitor (Perkin-Elmer), 2.5 μM oligo(dT)-primer, and 1 μg of total RNA in 40 μl. PCR was performed with 3 μl cDNA from the reverse transcription reaction, 1.5 mM $MgCl_2$, 2.5 μl PCR buffer II, 2.5 mM (each) dA/C/G/TTP, 10 pmol forward (mmOCLN FOR2 5′-GGCTCGGCAGGTTCGCTTATCT-3′, mmOCLN FOR3 5′-TTGGGACAGAGGCTATGG-3′, mmOCLN FOR4 5′-TGCCTCCACCCCCATCTG-3′), 10 pmol reverse (mmOCLN REV 2 5′-CCTTCTCCCGCAACTGGCATCT-3′, mmOCLN REV 3 5′-ACCCACTCTTCAACATTGGG-3′, mmOCLN REV 4 5′-AGGTTTCCGTCTGTCA-TAGTCTCC-3′) primer, and 1 unit AmpliTaq DNA polymerase (Perkin-Elmer) in 25 μl (5 min 95 °C, 20 s 95 °C, 30 s 60 °C, 30 s 72 °C, 35 cycles, 7 min 72 °C). PCR products were separated on 1% agarose gels (visualized by ethidium bromide).

### 2.10. Immunoblotting

Tissue was homogenized on iced lysate buffer with 20 mM Tris pH 7.4, 5 mM $MgCl_2$, 1 mM EDTA, 0.3 mM EGTA, 1 μl/ml aprotinin, 16 μg/ml benzamidine–HCl, 10 μg/ml phenanthroline, 10 μg/ml leupeptin, 10 μg/ml pepstatin, 1 mmol PMSF, 210 μg/ml sodiumfluoride, 2.16 mg/ml β-glycerophosphate, 18.5 μg/ml $NaVO_4$ and trypsin inhibitor 1 μl/ml (all substances obtained from Sigma Chemicals, St. Louis, MO). Insoluble material was removed at 200×$g$ for 5 min at 4 °C. Supernatants were then centrifuged at 43,000×$g$ for 30 min at 4 °C and the pellets representing a crude membrane fraction was resuspended in a lysate buffer. Protein was determined by Pierce BCA assay. 5 μg protein was separated by polyacrylamide gel electrophoresis and transferred to a PVDF membrane (NEN™, Boston, MA). Blots were blocked for 2 h in 5% milk powder and 2 h in bovine serum albumin before incubation with rabbit polyclonal IgG antibodies against the 150 carboxy-terminal amino acids of the occludin protein (1:10,000) or claudin-1 (1:5,000). Antibodies were from Zymed, South San Francisco, CA. POD-conjugated goat anti-rabbit IgG antibody and the chemiluminescence detection system Lumi-Light$^{PLUS}$ Western blotting kit (Boehringer Mannheim, Germany) were used to detect bound antibody.

### 2.11. Statistical analysis

Data are means±S.E. Group differences were tested by analysis of variance (ONE WAY ANOVA; Student–New-

Table 1
$Na^+$ and mannitol fluxes in the small and large intestines

| | $R^t$ | $I_{SC}$ | $J^{sm}_{Na}$ | $J_{mannitol}$ | $n$ |
|---|---|---|---|---|---|
| *Small intestine* | | | | | |
| Control | 36±5 | 5.0±1.1 | 16.0±2.4 | 0.34±0.04 | 8 |
| *occludin+/–* | 46±4$^{NS}$ | 2.3±0.5* | 13.2±1.6$^{NS}$ | 0.27±0.04$^{NS}$ | 8 |
| *occludin−/–* | 45±5$^{NS}$ | 3.0±0.8* | 12.2±2.1$^{NS}$ | 0.27±0.05$^{NS}$ | 8 |
| *Large intestine* | | | | | |
| Control | 64±3 | 2.8±0.4 | 7.1±0.1 | 0.12±0.02 | 8 |
| *occludin+/–* | 75±5$^{NS}$ | 2.9±0.3$^{NS}$ | 7.0±0.4$^{NS}$ | 0.10±0.02$^{NS}$ | 8 |
| *occludin−/–* | 68±2$^{NS}$ | 4.0±0.7$^{NS}$ | 6.8±0.4$^{NS}$ | 0.08±0.01$^{NS}$ | 9 |

Total tissue resistance ($R^t$) is in Ω cm$^2$. Short-circuit current ($I_{SC}$), serosal to mucosal $^{22}$Na fluxes ($J^{sm}_{Na}$), and mucosal-to-serosal [$^3$H]mannitol fluxes ($J_{mannitol}$) are in μmol h$^{-1}$ cm$^{-2}$. All values are means±S.E. *=<0.05, NS=not significantly different from control.

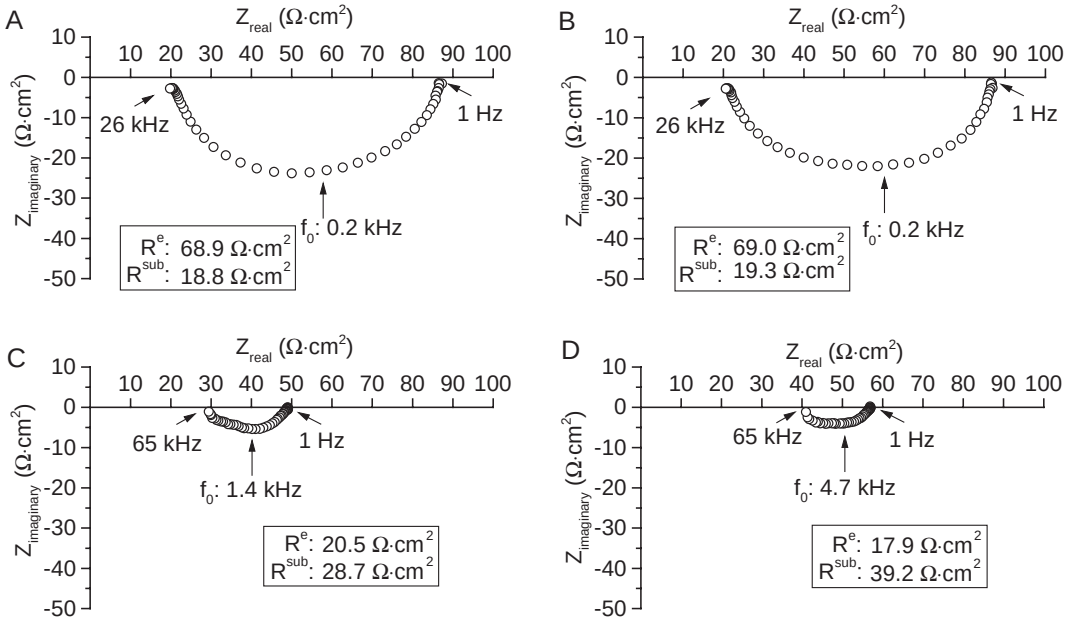


Fig. 1. Transmural electrical impedance of *occludin*-deficient mouse intestine. (A and C) Distal colon and jejunum from *occludin*+/+ control mice; (B and D) Distal colon and jejunum from *occludin*−/− mice. $Z_{real}$ gives the ohmic component and $Z_{imaginary}$ the reactive component of the complex impedance. Intersections between impedance locus and X-axis at low and high frequencies represent total tissue resistance ($R^t$) and subepithelial resistance ($R^{sub}$), respectively. $R^t$ minus $R^{sub}$ gives the resistance of the epithelium ($R^e$). For a detailed explanation of transepithelial impedance analysis see Refs. [13–15].

man–Keuls; $P<0.05$ was considered significant) using the SPSS for Windows software package. In case of significant difference, significance level was determined by two-tailed Student's *t*-test for unpaired data.

## 3. Results

### 3.1. Total resistance ($R^t$), short circuit current ($I_{SC}$), $^{22}Na$ flux ($J^{sm}_{Na}$) and [$^3$H]mannitol flux ($J_{mannitol}$)

Data are given in Table 1. Neither in *occludin*−/− mice nor in heterozygotic *occludin*+/− mice were significant changes in total resistance, serosal-to-mucosal sodium flux or mannitol flux detected. To exclude that an increase in anion and a decrease in cation conductance (or vice versa) compensated for each other, s-to-m $^{22}Na$ flux measurements were performed which are considered to reflect paracellular cation movement.

In contrast, small intestinal $I_{SC}$ showed a 40% decrease in homozygotic *occludin*−/− and a 54% decrease in heterozygotic *occludin*+/− mice. The ionic basis of $I_{SC}$ in the jejunum of control mice has been shown to represent electrogenic chloride secretion [22]. While the functional meaning of this decrease needs a more detailed discussion, it can at least be stated here that an influence on $R^t$ is not likely in the very leaky small intestine, in which the paracellular is much more conductive than the transcellular route.

### 3.2. Epithelial ($R^e$) and subepithelial ($R^{sub}$) resistance in the small and large intestines

Typical colonic impedance locus plots from *occludin*+/+ and *occludin*−/− mice are shown in Fig. 1. The data are presented in Table 2. In the distal colon of *occludin*+/+ mice, $R^e$ was 66±5 Ω cm$^2$ and $R^e$ contributed 77±3% to the total tissue resistance. In *occludin*−/− mice, $R^e$ was not significantly different (65±2 Ω cm$^2$) and this held true also in heterozygotic *occludin* deficiency (69±3 Ω cm$^2$). Also, the ratio of epithelial and total wall resistance ($R^e/R^t$) was not significantly different in homozygotic and heterozygotic *occludin*-deficient mice when compared to littermate con-

Table 2
Epithelial-to-total resistance ratio ($R^e/R^t$) in small and large intestine and gastric corpus mucosa

| | Small intestine | | | Large intestine | | | Stomach | | |
|---|---|---|---|---|---|---|---|---|---|
| | $R^e$ | $R^e/R^t$ | *n* | $R^e$ | $R^e/R^t$ | *n* | $R^e$ | $R^e/R^t$ | *n* |
| Control | 23±5 | 39±2% | 6 | 66±5 | 77±3% | 6 | 33±6 | 48±4% | 5 |
| *occludin (+/−)* | 24±4$^{NS}$ | 33±3%$^{NS}$ | 8 | 69±3$^{NS}$ | 82±1%$^{NS}$ | 7 | – | – | – |
| *occludin (−/−)* | 19±2$^{NS}$ | 35±1%$^{NS}$ | 9 | 65±2$^{NS}$ | 77±1%$^{NS}$ | 9 | 34±4$^{NS}$ | 54±7%$^{NS}$ | 4 |

Epithelial ($R^e$, Ω cm$^2$) and total tissue resistance ($R^t$, Ω cm$^2$) of proximal small and distal large intestine and gastric corpus as determined by alternating current impedance analysis. All values are means±S.E. NS=not significantly different from homozygotic *occludin* control.

trols. A similar result was obtained also in the small intestine: $R^e$ was 23±5 Ω cm$^2$ in the control and contributed 39±2% to total resistance, a ratio as low as expected for the leaky small intestine, and neither in homozygotic nor in heterozygotic *occludin*-deficient mice had $R^e$ significantly changed.

### 3.3. Conductance scanning in distal colon

The data are given in Table 3. In control littermates, the surface epithelium contributed 7.1±0.8 mS/cm$^2$ and the crypt epithelium 1.9±0.4 mS/cm$^2$ to the total tissue conductivity of 9.0±0.8 mS/cm$^2$. No significant difference was obtained in homozygotic (−/−) or heterozygotic (+/−) *occludin*-deficient mice. This rules out that opposite changes of conductivity in surface and crypt epithelia compensate each other and escape the detection by conventional resistance measuring techniques.

To exclude a concomitant opposite change in transcellular and tight junctional (paracellular) conductance which compensate each other, we distinguished trans- ($G^c$) and paracellular ($G^{tj}$) pathways in the conductivity of surface epithelium ($G^{se}$) (Table 3). In the control, $G^c$ contributed 7.6±1.0 mS and $G^{tj}$ 0.3±0.1 mS to the overall surface conductance. The $G^{tj}$ being relatively small, i.e. only about 3% of $G^{se}$, indicates a medium tight epithelium.

Table 3
Electrical conductivity in mouse distal colon and urinary bladder

(A) Contribution of surface epithelium ($G^{se}$) and crypts ($G^{cry}$) to total conductivity ($G^t$)

| | $G^t$ | $G^{se}$ | $G^{cry}$ | $n$ |
|---|---|---|---|---|
| Control | 9.0±0.8 | 7.1±0.8 | 1.9±0.4 | 8 |
| *occludin*+/− | 9.4±1.4$^{NS}$ | 7.3±1.1$^{NS}$ | 2.1±0.5$^{NS}$ | 8 |
| *occludin*−/− | 8.7±0.7$^{NS}$ | 6.8±0.5$^{NS}$ | 1.9±0.6$^{NS}$ | 8 |

(B) Contribution of transcellular ($G^c$) and paracellular pathway ($G^{tj}$) to $G^{se}$

| | $G^{se}$ | $G^c$ | $G^{tj}$ | $G^{tj}$ in % of $G^{se}$ | $n$ |
|---|---|---|---|---|---|
| Control | 7.9±0.9 | 7.6±1.0 | 0.3±0.1 | 4.1±1.3 | 6 |
| *occludin*+/− | 6.7±1.9$^{NS}$ | 6.5±1.9$^{NS}$ | 0.2±0.1$^{NS}$ | 4.0±1.4$^{NS}$ | 4 |
| *occludin*−/− | 7.3±0.7$^{NS}$ | 7.1±0.6$^{NS}$ | 0.2±0.1$^{NS}$ | 2.2±1.5$^{NS}$ | 5 |

(C) Transepithelial resistance ($R^t$) of urinary bladder, a tight epithelium

| | $R^t$ | $R^t_{min}$ | $n$ |
|---|---|---|---|
| Control | 5.8±0.8 | 3.3 | 5 |
| *occludin*+/− | 5.3±2.1$^{NS}$ | 2.4 | 5 |
| *occludin*−/− | 6.0±2.2$^{NS}$ | 2.3 | 5 |

Conductivities (mS/cm$^2$) in mouse distal colon. Note that $G^t=1/R^t$, $G^t=G^{se}+G^{cry}$, and $G^{se}=G^c+G^{tj}$. Data were measured by medium (A) or high resolution (B) *conductance scanning* [16]. (C) Transepithelial resistance ($R^t$) in kΩ cm$^2$ in urinary bladder. $R^t_{min}$ represents lowest single value of the respective group. Measurements were done by positioning an apical voltage-sensing electrode very close to the epithelium and in the center of the chamber opening, thus minimizing influences of "edge damage". All values are means±S.E. NS=not significantly different from control.

Table 4
Distension- and EGTA-induced changes in epithelial barrier and transport function in the large intestine

| | Distension | | | EGTA | | |
|---|---|---|---|---|---|---|
| | $R^t_{basal}$ | $R^t_{distension}$ | $n$ | $R^t_{basal}$ | $R^t_{EGTA}$ | $n$ |
| Control | 64±3 | 47±4 | 7 | 85±4 | 29±1 | 7 |
| *occludin*+/− | 57±4$^{NS}$ | 45±6$^{NS}$ | 8 | 91±4$^{NS}$ | 26±1$^{NS}$ | 6 |
| *occludin*−/− | 59±3$^{NS}$ | 50±3$^{NS}$ | 9 | 84±4$^{NS}$ | 35±6$^{NS}$ | 7 |

Total tissue resistance ($R^t$, in Ω cm$^2$) is given under basal conditions ($R^t_{basal}$) and 30 min after distension ($R^t_{distension}$) as well as before ($R^t_{basal}$) and after addition of EGTA ($R^t_{EGTA}$). All values are means±S.E. NS=not significantly different from control.

However, neither $G^c$ nor $G^{tj}$ were significantly different in homozygotic (−/−) or heterozygotic (+/−) *occludin*-deficient mice.

### 3.4. Colonic barrier function during mechanical stress and calcium depletion

In Table 4, the total tissue resistance is given under basal conditions ($R^t_{basal}$) and 30 min after distension ($R^t_{distension}$) as well as before ($R^t_{basal}$) and after the addition of EGTA ($R^t_{EGTA}$) which can open tight junctions. In the control, both perturbations reduced $R^t$. However, there was no significant difference in heterozygotic or homozygotic *occludin* deficiency.

### 3.5. Barrier function of urinary bladder epithelium

The electrical resistance of the urinary bladder, a very tight epithelium [23], was determined in the *conductance scanning* chamber to exclude edge damage contributions. In all homozygotic *occludin*-deficient mice as well as in all (+/+) littermate controls, the resistance exceeded 2 kΩ cm$^2$ and mean resistance was between 5 and 6 kΩ cm$^2$ (Table 3) with no significant difference between both groups.

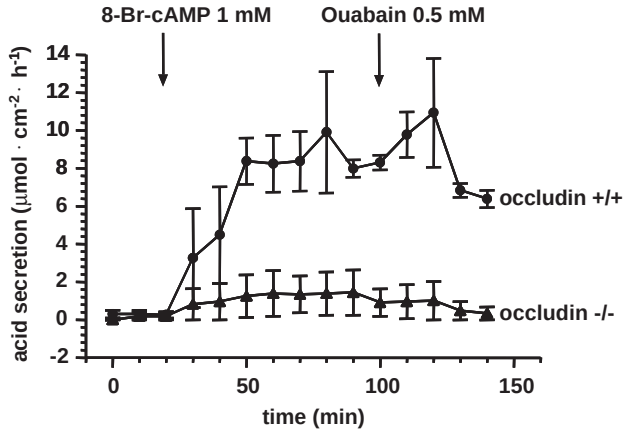


Fig. 2. Gastric acid secretion in antrum mucosa. Gastric acid secretion of homozygotic *occludin*-deficient mice and of corresponding (+/+) littermate controls was measured using the pH-stat method. All values are means± S.E. *=<0.05; NS=not significantly different from control.

### 3.6. Gastric acid secretion

The data are depicted in Fig. 2. Gastric acid secretion was almost abolished in homozygotic *occludin−/−* mice. This was paralleled by a dramatic change in gastric morphology with mucus cell hyperplasia and a loss of parietal cells. Color histographs from different ages of occludin-deficient mice have already been published [11].

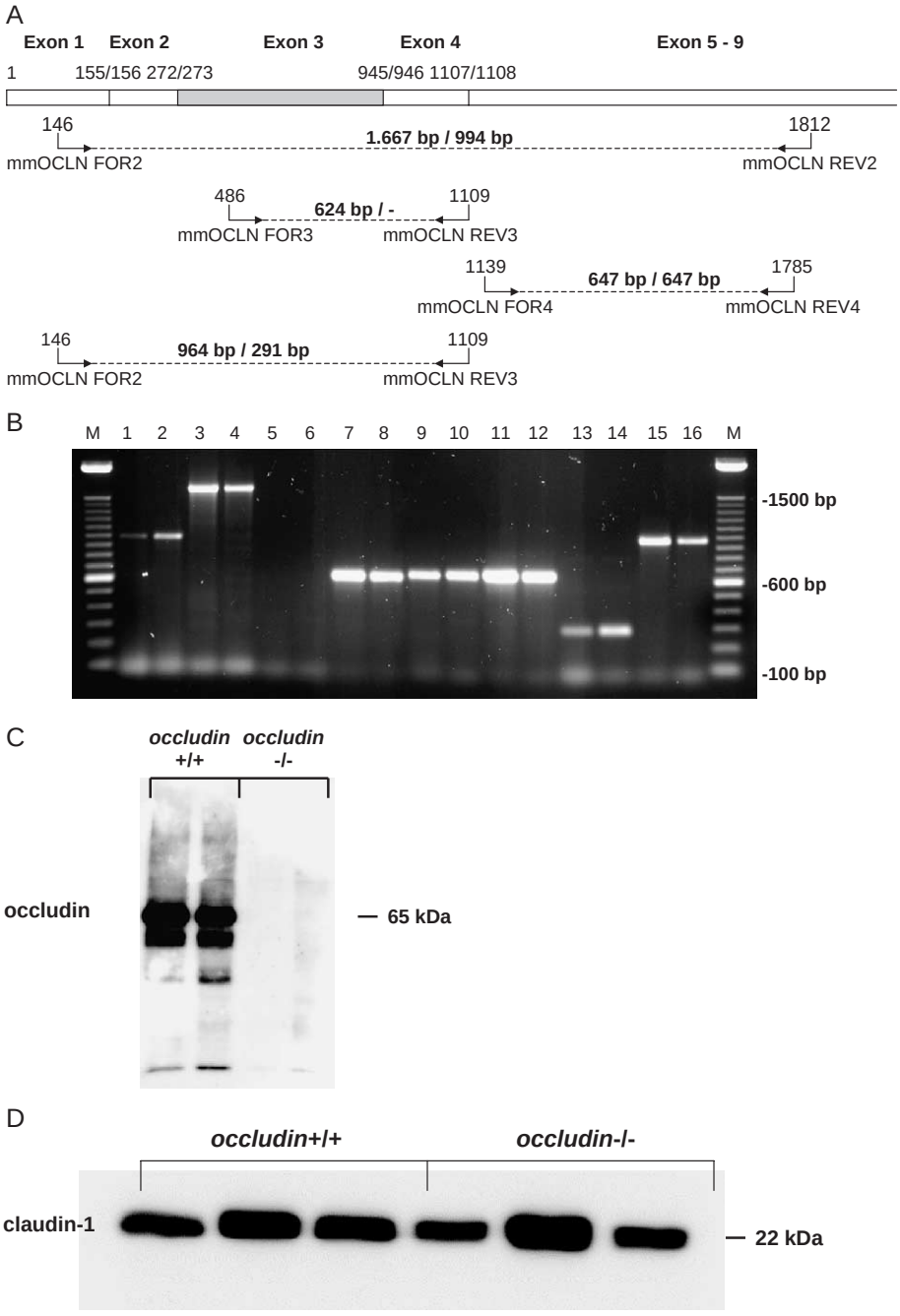


Fig. 3. Expression of *occludin* in wild-type and *occludin*-deficient mice. (A) Location of *occludin* specific oligonucleotides used for RT-PCR with respect to the exon/exon structure of murine *occludin* cDNA. The predicted length of amplification products from RNA of wild-type/*occludin−/−* mice is depicted with bold numbers. (B) Size distribution of PCR products after reverse transcription and amplification with primer pairs mmOCLNFOR2/REV2 (Lanes 1–4), mmOCLNFOR3/REV3 (Lanes 5–8), mmOCLNFOR4/REV4 (Lanes 9–12), and mmOCLNFOR2/REV3 (Lanes 13–16). RNA was derived from wild-type (Lanes 3 and 4, 7 and 8, 11 and 12, 15 and 16) and *occludin−/−* mice (Lanes 1 and 2, 5 and 6, 9 and 10, 13 and 14). M, Marker. (C) Immunodetection of *occludin* in protein extracts of colonic tissue from wild-type (Lanes 1 and 2) and *occludin−/−* mice (Lanes 3 and 4) using the Zymed rabbit polyclonal antibody directed against the 150 carboxy-terminal amino acids of the occludin protein. (D) Western blot of *claudin-1* in protein extracts from distal large intestine of *occludin−/−* mice and *occludin+/+* control littermates.

### 3.7. PCR and immunoblotting of occludin−/− tissue

To evaluate if downstream sequences were processed to mRNA in spite of the deletion covering exon 3 of the *occludin* gene, DNA fragments were amplified which overlap, include in part or are located downstream of the deleted region (Fig. 3A). As expected, primers located within the deleted region did not generate a PCR fragment (Fig. 3B, lanes 5 and 6). Primer pairs covering the deleted region generated a shorter DNA fragment from the RNA of homozygous knockout mice (Fig. 3B, lanes 1 and 2, 13 and 14). This indicates that primer binding sites downstream of the 673 bp deletion can be used for amplification after reverse transcription of RNA from homozygous *occludin*-knockout mice. However, the frame-shift introduced in the open reading frame by the deletion of exon 3 prevents the expression of an *occludin* with functional C-terminal sequences as proved by the immunodetection of *occludin* (Fig. 3C).

Furthermore, in immunoblots of distal colon, no change in *claudin-1* expression was detected in *occludin*−/− mice when compared to *occludin*+/+ littermate controls (Fig. 3D).

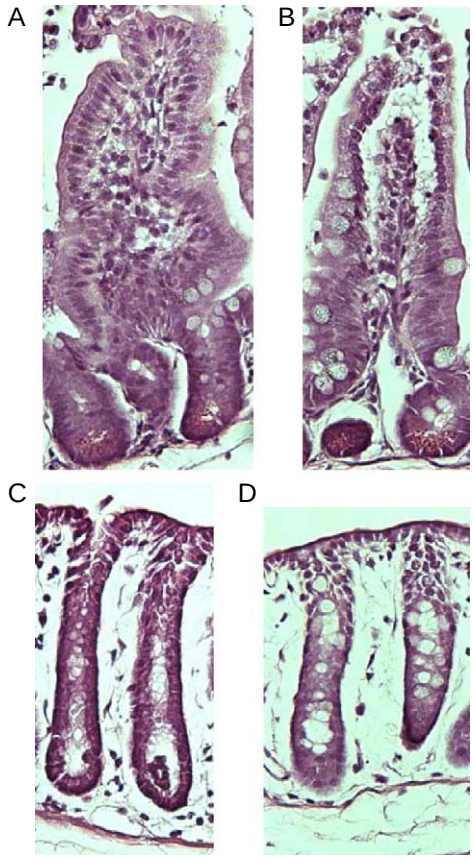


Fig. 4. Mucosal morphology. Mucosal architecture was not altered in small or large intestine of occludin-deficient mice. (A and B) Jejunum of occludin+/+ and occludin−/− mice. (C and D) Distal large intestine of occludin+/+ and occludin−/− mice (HE staining).

### 3.8. Mucosal morphology

For conventional histology 5 μm cross sections were stained with HE (Fig. 4). No structural changes were detected in occludin deficiency. Furthermore, colonic enterocyte height was unchanged (16±1 μm, $n$=4, in occludin−/− mice and 17±1 μm, $n$=4, in occludin+/+ controls, n.s.) and colonic enterocyte count per 100 μm crypt length was not altered (15.3±0.3, $n$=4, in occludin−/− mice and 14.8±0.5 in occludin+/+ controls, $n$=4, n.s.).

## 4. Discussion

The present paper aimed to characterize the functional role of *occludin*, the first tight junction strand protein discovered [6]. So far, experimental evidence seems to support a functional role as paracellular barrier molecule, namely (i) the influence of mutant and chimeric *occludin* expression on permeability of MDCK cells [24–26] and *Xenopus* embryonic epithelia [25], and (ii) its functional impairment with *occludin* homologous peptides in A6 cells [27,28]. For a more direct approach, the *occludin*-deficient mouse model [12] was used here.

Occludin-deficient mice were checked for the absence of occludin and its splice variants on mRNA and protein level with an antibody directed against the C-terminal 150 AA. The analysis of RNA from homozygous knockout mice revealed the expression of truncated occludin mRNA. However, the expression of occludin containing wild-type C-terminal AA sequences was not detected by an antibody directed against the C-terminal 150 AA. This can be explained by the deletion of exon 3 which leads to a frame-shift in the occludin open reading frame [11]. Recently, a variant of occludin with an altered N-terminal sequence was found in MDCK cells [29] and our group has published 3 splice variants [30]. However, our results give no evidence that splice variants are expressed in occludin-deficient mice, which can substitute for wild-type occludin.

The influence of *occludin* deficiency on epithelial barrier function was evaluated by several measuring techniques in different segments along the GI tract, and in urinary bladder as a very tight epithelium. Mannitol flux is assumed to reflect paracellular permeability. Sodium s-to-m flux and conductance measurements reflect either the paracellular route (small intestine), the transcellular route (urinary bladder) or both routes (in the intermediate tight large intestine and gastric mucosa). It turned out that functional parameters were *not* affected in *occludin*-deficiency, even in the urinary bladder which possesses an extremely tight epithelium. However, one has to keep in mind that a "negative result" can never rule out that a barrier dysfunction is present which is not detectable with our experimental design.

Therefore, we went on with our search for barrier defects in occludin deficiency by using more refined techniques.

Analysis of the spatial distribution of ionic permeability was performed by *conductance scanning*. Thus, we discriminated crypt and surface conductivity in distal colon. Regarding the life span of intestinal epithelial cells (and their tight junctions), crypts are composed of younger immature cells, while the surface epithelium possesses fully developed enterocytes. Hence, this discrimination would detect also small proliferation-dependent changes but no significant change could be found.

To exclude that *occludin* deficiency has caused regulatory changes in the transcellular route which could have superposed changes in paracellular conductance, the *conductance scanning* method was applied. It turned out that the ionic permeability of the tight junctions, assessed by the conductivity of the paracellular pathway ($G^{tj}$) in colonic surface epithelium, was not different in *occludin*-deficient mice.

To exclude that tight junctions become functionally handicapped when exposed to mechanical or chemical stress, resistance measurements were performed also during perturbation of the barrier. Neither a distension protocol nor chemical stress by a low calcium switch revealed any difference in homozygotic *occludin*-deficient mice. Calcium switch from a concentration of 1.2 mM to 0.3 μM by means of EGTA in serosal compartment is an established method for labializing tight junctions and is assumed to affect tight junctional permeability for ions by interfering with the binding of tight junction proteins with each other.

While *occludin* deficiency did not cause a detectable alteration of barrier function, alterations of transport functions were observed, especially in gastric mucosa. Structural changes have already been described in gastric corpus [12], which do not represent chronic inflammation as originally hypothesized but rather altered differentiation with subsequent chief and parietal cell reduction and mucus cell hyperplasia. As early as 6 weeks after birth, the number of chief and parietal cells is strongly decreased. At later stages, the area in which the parietal and surface cells normally reside is filled with unclassifiable epithelial cells. Thereafter, severe inflammatory changes are seen. However, the early loss of specific cells suggests a defect in differentiation as primary defect. Since gastric inflammation is also seen in other knockout mouse models with a primary defect in acid secretion, it seems to follow loss of functionality. Curious as to the function of this epithelium, we found a complete lack of basal and stimulated acid secretion. Interestingly, basal $HCO_3^-$ secretion was also not increased. Although the molecular basis for these changes are yet unknown, they indicate that *occludin* may be involved in the process of cellular differentiation in some but not all organs, since the small and large intestines were not affected.

In addition, a lower electrogenic ion transport in the small intestine of *occludin*-deficient mice was detected. Whether this represents a stimulatory influence of *occludin* on transporters or on activating signal transduction pathways is not clear from the present data. But again, as in the stomach, this influence on transport activity takes place without any barrier effect.

Taken together, this paper presents evidence against an essential role of *occludin* for the barrier formation within the epithelial tight junction strand heteropolymer. In contrast to *claudin-1*-deficient mice which die due to a massive loss of electrolytes and water through the functionally handicapped skin barrier [32], *occludin* deficiency is less deleterious. However, the exact role of single tight junctional strand components is still far from being clear. That resistance did not change in *occludin* deficiency together with proliferative alterations in the gastric mucosa could also point to a regulatory function of *occludin*. Alternatively, tight junction strands could be composed as a heteropolymer of several different protein components, some of which are not essential or can at least be substituted for by others like e.g. by claudins. This also means that epithelial barrier dysfunction caused by the down-regulation of tight junction proteins, as e.g. when *occludin* expression is reduced in response to pro-inflammatory cytokines [31], does not only require the down-regulation of one tight junction protein as *occludin* but that one has also to assume direct or indirect effects on other tight junction strand components simultaneously. However, checking the expression level of *claudin-1* in our *occludin*-deficient mice revealed no up- or down-regulation which could have compensated for a functional loss of *occludin*.

## Acknowledgement

This study was supported by grants from Deutsche Forschungsgemeinschaft (Schu 559/7-1 and 7-3, Fr 652/4-1 and -2, and Se 460/13-2 and 9-4), from the Else Kröner-Fresenius-Stiftung and the Mednet of inflammatory bowel disease. The excellent assistance of Anja Fromm, Sieglinde Lüderitz, and Susanna Schön, and the great support of the electronic engineer Detlef Sorgenfrei are gratefully acknowledged.

## References

[1] P. Claude, Morphological factors influencing transepithelial permeability: a model for the resistance of the zonula occludens, J. Membr. Biol. 39 (1978) 219–232.

[2] H. Schmitz, M. Fromm, J.C. Bentzel, P. Scholz, K. Detjen, J. Mankertz, H. Bode, H.J. Epple, E.O. Riecken, J.D. Schulzke, Tumor necrosis factor-alpha (TNFα) regulates the epithelial barrier in the human intestinal cell line HT-29/B6, J. Cell. Sci. 112 (1999) 137–146.

[3] M.E. Duffey, B. Hainau, S. Ho, C.J. Bentzel, Regulation of epithelial tight junction permeability by cyclic AMP, Nature 294 (1981) 451–453.

[4] G. Conyers, L. Milks, M. Conklyn, H. Showell, E. Cramer, A factor in serum lowers resistance and opens tight junctions of MDCK cells, Am. J. Physiol. 259 (1990) C577–C585.

[5] A. Fasano, B. Baudry, D.W. Pumplin, S.S. Wasserman, B.D. Tall, J.M. Ketley, J.B. Kaper, Vibrio cholerae produces a second enterotoxin which affects intestinal tight junctions, Proc. Natl. Acad. Sci. U. S. A. 88 (1991) 5242–5246.
[6] M. Furuse, T. Hirase, M. Itoh, A. Nagafuchi, S. Yonemura, S. Tsukita, S. Tsukita, Occludin: a novel integral membrane protein localizing at tight junctions, J. Cell Biol. 123 (1993) 1777–1788.
[7] M. Furuse, M. Itoh, T. Hirase, A. Nagafuchi, S. Yonemura, S. Tsukita, S. Tsukita, Direct association of occludin with ZO-1 and its possible involvement in the localization of occludin at tight junctions, J. Cell Biol. 127 (1994) 1617–1626.
[8] K. Morita, M. Furuse, K. Fujimoto, S. Tsukita, Claudin multigene family encoding four-transmembrane domain protein components of tight junction strands, Proc. Natl. Acad. Sci. U. S. A. 96 (1999) 511–516.
[9] S. Tsukita, M. Furuse, M. Itoh, Multifunctional strands in tight junctions, Nat. Rev., Mol. Cell Biol. 2 (2001) 285–293.
[10] I. Martin-Padure, S. Lostaglio, M. Schneemann, L. Williams, M. Romano, P. Fruscella, C. Panzeri, A. Stoppacciaro, L. Ruco, A. Villa, D. Simmons, E. Dejana, Junctional adhesion molecule, a novel member of the immunoglobulin superfamily that distributes at intercellular junctions and modulates monocyte transmigration, J. Cell Biol. 142 (1998) 117–127.
[11] M. Saitou, K. Fujimoto, Y. Doi, M. Itoh, T. Fujimoto, M. Furuse, H. Takano, T. Noda, S. Tsukita, Occludin-deficient embryonic stem cells can differentiate into polarized epithelial cells bearing tight junctions, J. Cell Biol. 141 (1998) 397–408.
[12] M. Saitou, M. Furuse, H. Sasaki, J.D. Schulzke, M. Fromm, H. Takano, T. Noda, S. Tsukita, Complex phenotype of mice lacking occludin, a component of tight junction strands, Mol. Biol. Cell 11 (2000) 4131–4142.
[13] M. Fromm, J.D. Schulzke, U. Hegel, Epithelial and subepithelial contributions to transmural electrical resistance of intact rat jejunum, in vitro, Pflügers Arch. 405 (1985) 400–402.
[14] J.D. Schulzke, M. Fromm, U. Hegel, Epithelial and subepithelial resistance of rat large intestine: segmental differences, effect of stripping, time course, and action of aldosterone, Pflügers Arch. 407 (1986) 632–637.
[15] A.H. Gitter, J.D. Schulzke, D. Sorgenfrei, M. Fromm, Ussing chamber for high-frequency transmural impedance analysis of epithelial tissues, J. Biochem. Biophys. Methods 35 (1997) 81–88.
[16] A.H. Gitter, M. Bertog, J.D. Schulzke, M. Fromm, Measurement of paracellular epithelial conductivity by conductance scanning, Pflügers Arch. 434 (1997) 830–840.
[17] J.D. Schulzke, M. Fromm, C.J. Bentzel, M. Zeitz, H. Menge, E.O. Riecken, Ion transport in the experimental short bowel syndrome of the rat, Gastroenterology 102 (1992) 497–504.
[18] H. Schmitz, C. Barmeyer, M. Fromm, N. Runkel, H.D. Foss, C.J. Bentzel, E.O. Riecken, J.D. Schulzke, Altered tight junction structure contributes to the impaired epithelial barrier function in ulcerative colitis, Gastroenterology 116 (1999) 301–309.
[19] A. Köckerling, D. Sorgenfrei, M. Fromm, Electrogenic $Na^+$ absorption of rat distal colon is confined to surface epithelium. A voltage scanning study, Am. J. Physiol. 264 (1993) C1285–C1293.
[20] A. Köckerling, M. Fromm, Origin of cAMP dependent $Cl^-$ secretion from both crypts and surface epithelia of rat intestine, Am. J. Physiol. 264 (1993) C1294–C1301.
[21] J.D. Schulzke, E.O. Riecken, M. Fromm, Distension-induced electrogenic $Cl^-$ secretion is mediated via VIP-ergic neurons in rat rectal colon, Am. J. Physiol. 268 (1995) G725–G731.
[22] B.R. Grubb, Ion transport across the jejunum in normal and cystic fibrosis mice, Am. J. Physiol. 268 (1995) G505–G513.
[23] S.A. Lewis, Everything you wanted to know about the bladder epithelium but were afraid to ask, Am. J. Physiol., Renal Physiol. 278 (2000) F867–F874.
[24] M.S. Balda, J.A. Whitney, C. Flores, S. Gonzales, M. Cereijido, K. Matter, Functional dissociation of paracellular permeability and transepithelial electrical resistance and disruption of the apical–basolateral intramembrane diffusion barrier by expression of a mutant tight junction membrane protein, J. Cell Biol. 134 (1996) 1031–1049.
[25] Y. Chen, C. Merzdorf, D.L. Paul, D.A. Goodenough, COOH terminus of occludin is required for tight junction barrier function in early *Xenopus* embryos, J. Cell Biol. 138 (1997) 891–899.
[26] M.S. Balda, C. Flores-Maldonado, M. Cereijido, K. Matter, Multiple domains of occludin are involved in the regulation of paracellular permeability, J. Cell. Biochem. 78 (2000) 85–96.
[27] V. Wong, B.M. Gumbiner, A synthetic peptide corresponding to the extracellular domain of occludin perturbs the tight junction permeability barrier, J. Cell Biol. 136 (1997) 399–409.
[28] F. Lacaz-Vieira, M.M. Jaeger, P. Farshori, B. Kachar, Small synthetic peptides homologous to segments of the first external loop of occludin impair tight junction resealing, J. Membr. Biol. 168 (1999) 289–297.
[29] Z. Muresan, D.L. Paul, D.A. Goodenough, Occludin 1B, a variant of the tight junction protein occludin, Mol. Biol. Cell 11 (2000) 627–634.
[30] J. Mankertz, S.J. Waller, B. Hillenbrand, S. Tavalali, P. Florian, T. Schöneberg, M. Fromm, J.D. Schulzke, Gene expression of the tight junction protein occludin includes differential splicing and alternative promoter usage, Biochem. Biophys. Res. Commun. 298 (2002) 657–666.
[31] J. Mankertz, S. Tavalali, H. Schmitz, A. Mankertz, E.O. Riecken, M. Fromm, J.D. Schulzke, Expression from the human occludin promoter is affected by tumor necrosis factor alpha and interferon gamma, J. Cell. Sci. 113 (2000) 2085–2090.
[32] M. Furuse, M. Hata, K. Furuse, Y. Yoshida, A. Haratake, Y. Sugitani, T. Noda, A. Kubo, S. Tsukita, Claudin-based tight junctions are crucial for the mammalian epidermal barrier: a lesson from claudin-1-deficient mice, J. Cell Biol. 156 (2002) 1099–1111.